DOI: 10.17725/rensit.2021.13.471

Hybrid superconducting heterostructures with magnetic interlayers

Karen Y. Constantinian, Gennady A. Ovsyannikov, Yulii V. Kislinski, Andrey M. Petrzhik
Kotelnikov Institute of Radioengineering and Electronics of RAS, http://www. cplire.ru/
Moscow 125009, Russian Federation
E-mail: karen@hitech.cplire.ru, gena@hitech.cplire.ru, yulii@hitech.cplire.ru, petrzhik@hitech.cplire.ru
Anton V. Shadrin
Moscow Institute of Physics and Technology, https://mipt.ru/
Dolgoprudny 141701, Moscow Region, Russian Federation
E-mail: anton_sh@hitech.cplire.ru
Alexei S. Kalaboukhov
Chalmers University of Technology, https://www.chalmers.se/
SE-412 96 Göteborg, Sweden
E-mail: alexei.kalaboukhov@chalmers.se
Received Oktober 20, 2021, peer-reviewed Oktober 27, 2021, accepted November 08, 2021

Abstract: **Electron transport processes in oxide superconducting heterostructures with epitaxially grown magnetic thin-film interlayers, in which the interaction of superconducting correlations and magnetic ordering occurs due to superconducting and magnetic proximity effects, have been studied experimentally. Hybrid mesa-heterostructures were prepared from thin-film bottom cuprate superconductor (S), magnetic (M) interlayer made of manganite or an antiferromagnetic cuprate, and the upper electrode made from an ordinary superconductor. When the cuprate antiferromagnetic material was replaced by a ferromagnetic manganite interlayer, the superconducting current was suppressed, although the thin magnetic film was several times thinner, 5 nm, and the temperature was lowered to 0.3 K. At low temperatures dependences of differential resistance vs. voltage for mesa-heterostructures with manganite interlayer featured mini-gap low-energy states.**

Keywords: **superconducting heterostructures, thin films, manganites, cuprates, differential conductivity, exchange energy**

PACS: 74.45.+c, 74.72.−h, 75.47.Lx, 73.63.−b

Acknowledgments: This work was supported by the Ministry of Science and Higher Education of the Russian Federation (Agreement No. 075-15-2021-990).

For citation: Karen Y. Constantinian, Gennady A. Ovsyannikov, Anton V. Shadrin, Yulii V. Kislinski, Andrey M. Petrzhik, Alexei S. Kalaboukhov. Hybrid superconducting heterostructures with magnetic interlayers. *RENSIT: Radioelectronics. Nanosystems. Information technologies*, 2021, 13(4)471-478. DOI: 10.17725/rensit.2021.13.471.

Contents

1. INTRODUCTION

The coexistence of superconducting and magnetic ordering leads to an unusual behavior of the superconducting pair potential. In ferromagnetic (*F*) and superconducting (*S*) junctions the oscillatory behavior of the paired potential took place [1,2], and as a consequence, a π-state occurs in *S*/*F*/*S* structures as predicted in [3] and experimentally confirmed on niobium superconducting structures with copper-nickel interlayers [4]. The interest to *S*/*F*/*S* structures is caused by opportunities of obtaining non-sinusoidal current-phase relation, π-junctions, systems with spin valve properties, electronic transport with spin-triplet superconducting correlations with nonzero spin projection, long-range proximity effect and a number of other effects.

A lot number of papers have been devoted to the physical mechanisms for the development of *S*/*F*/*S* structures with metallic F-layers (see, for example, reviews [5,6]). The case of the *S*/*AF* boundary formed between a superconductor and an antiferromagnet (*AF*) is no less interesting [7-9]. However, the creation of structures based on metallic layers with *S, F* and *AF* properties encountered technological problems, the solution of which are associated with the design and development of technology of heterostructures fabrication with epitaxially grown interfaces between thin films of oxide materials with the required functionalities.

Note, when polycrystalline films are used for preparation of *F*/*S* interfaces, the influence of the crystal structure on contacting materials leads to that a number of interesting effects cannot be observed. For example, the anomalously strong proximity effect was absent in the junctions with the *AF* interlayers, which manifests itself in a magnetic layered structure with the *AF* ordering of interlayer [7,8].

A number of specific properties of manganites [10] and antiferromagnetic cuprates have led to increasing interest in heterostructures with epitaxially grown interlayers of magnetically active materials characterized by identical crystal structure and similar crystallographic parameters. As shown in [11,12], thin-film interfaces of manganite/superconducting cuprate $La_{0.7}Ca_{0.3}MnO_3/YBa_2Cu_3O_x$ (LCMO/YBCO) or $La_{0.7}Sr_{0.3}MnO_3/YBa_2Cu_3O_x$ (LSMO/YBCO) can be made very smooth on atomic level and free of defects. Chemical diffusion of the boundary elements was absent within the experimental error, and measurements [13] showed a minor migration of manganese ions within 1 nm. The high degree of polarization of manganites indicates that superconducting structures containing manganite interlayers with ferromagnetic ordering, as well as antiferromagnetic oxides, are very interesting for studies of spin-dependent electronic transport and proximity effects in multilayer heterostructures.

This paper presents the results of experimental studies of hybrid $S/M/S_d$ mesa-heterostructures (MHS) Nb/Au/M/$YBa_2Cu_3O_x$ in which an Nb/Au bilayer was used as the *S* superconductor with *s*-symmetry of order parameter and an epitaxial film of $YBa_2Cu_3O_x$ (YBCO) superconducting cuprate with a dominant order parameter with *d*-wave symmetry, used as the S_d superconductor. The magnetically active layer (*M*) was prepared from a manganite

film with optimal $La_{0.7}Ca_{0.3}MnO_3$ doping, or from non-doped manganite film $LaMnO_3$. The optimal doping level means the level of doping at which the Curie temperature is maximal.

The results of resistivity measurements of MHS with manganite interlayers at low temperatures T = 2 K, 1 K and 0.3 K will be compared to the dependences obtained in [14], calculated taking into account the impact of exchange interaction energy h. Another type of MHS studied in this work has the *M*-layer material made from antiferromagnetic $Ca_XSr_{1-X}CuO_2$ cuprate with doping level x = 0.5 (CSCO).

2. EXPERIMENTAL MESA-HETEROSTRUCTURES

The superconducting cuprate YBCO film with critical temperature T_C = 88-89 K was prepared by laser ablation at 700-800°C and pressure 0.3 mbar on (110)$NdGaO_3$ (NGO) substrate. A thin d_M = 5...20 nm manganite *M*-layer film was epitaxially grown in the same vacuum chamber at high temperature and then coated with a thin (20-30 nm) gold (Au) layer after cooling to room temperature. A subsequent layer of niobium (Nb) was deposited by magnetron sputtering. The protective Au film used to reduce oxygen diffusion from the contacting oxides. The proximity effect between the superconducting (Nb) and metallic (Au) films gave the critical bilayer temperature $T_{C'}$ = 8.5...9 K, close to the critical temperature of the Nb film (9.2 K). The LCMO *M*-layer manganite thin film at temperatures T < 100 K has the properties of a ferromagnetic metal. In the case of manganite $LaMnO_3$ very thin *M*-layer at low temperatures may exhibit properties of an antiferromagnet [10,13], however, at thicknesses which exceed the thickness of pin-holes (d_M > 1 nm) it becomes a weak ferromagnet.

The topology of the mesa-heterostructures was formed by photolithography, plasma-chemical, and ion-beam etching methods [15]. A protective layer of SiO_2 insulator was deposited by high-frequency magnetron sputtering and then a square-shaped planar geometry was formed, defining the *MHS* area varied from A = 10×10 μm² to 50×50 μm². For comparison, a similar fabrication procedure was used for structures without *M*-layer [16]. To avoid the appearance of pin-holes (short circuits for electric current), the deposited *M* films were thicker than the surface roughness of the YBCO layer. Direct deposition of Nb on top of the YBCO film results in an Nb/YBCO interface with high resistivity due to oxidation of the Nb film. Thus, if the Au layer locally damaged due to the finite surface roughness of the M/S_d interface, then niobium oxide is formed directly there, which prevents pin-hole formation.

3. RESULTS OF MEASUREMENTS AND DISCUSSION

3.1. Specific resistance of MHS with manganite interlayers

The temperature dependences of the resistivity of epitaxial LMO and LCMO films deposited on NGO substrate were investigated [15] to evaluate their contribution to the *MHS* resistivity. Note that the resistance of the LMO film is much higher than that of the doped ferromagnetic manganite film, particularly, the LCMO. The increase in resistance with decreasing temperature indicates nonmetallic conductivity.

A detailed analysis of the temperature dependence shows that on the dependence $R(T)$ the Mott insulator behavior with two

components can be distinguished, which are described by an expression $\rho \infty \exp(T_0/T)^{1/4}$ with different characteristic temperatures $T_0 = 34 \cdot 10^6$ K at $T > T_{CU}$ and $T_0 = 4 \cdot 10^6$ K at $T < T_{CU}$, where T_{CU} is the Curie phase transition temperature. The difference in T_0 parameter below and above T_{CU} can be described using a polaron model of hopping conduction at high temperature [16] for which the dependence $\rho = \alpha \exp(T_0^*/T)^{1/4}$, where T_0^* is the activation temperature and the parameter α depends on the concentration of charge carriers and the jump length.

The *MHS* resistance is described by sum of resistances $R = R_{YBCO} + R_{M/Y} + R'_M + R_b + R_{Nb/Au} + R_{Nb} + R_{Au}$, where R_{YBCO} is the YBCO electrode resistance, $R_{M/Y}$ is the M/YBCO interface resistance, R'_M is the *M*-layer resistance, R_b is the Au/M barrier resistance, and R_{Nb} and R_{Au} are the Nb electrode and Au film resistances, respectively. Usually, the contribution from the Au thin film resistance can be neglected [16].

At temperatures above the superconducting critical temperature (T_C = 70÷80 K) of the YBCO film ($T > T_C$), the temperature dependence of the MHS resistance $R(T)$ is similar to that of a single YBCO film. MHS with *M*-layer of a manganite film had no superconducting critical current, although the thickness d_M was reduced to 5 nm. In the case of LSMO manganite *M*-layer its impedance in MHS, calculated from the resistivity of the single film, is much higher than the total impedance of the MHS. Consequently, there is a significant decrease in the resistivity of the M-layer in the MHS.

Taking the calculated maximum resistance of the interface between Au and manganite and assuming that the contribution of the *M*-layer resistance is insignificant, we find that the determining factor in the MHS resistance comes from the manganite/YBCO interface. **Fig. 1** shows the family of dependences of characteristic resistances $R_N A(V)$ for MHS with an LMO layer with thickness d_M = 6 nm and size L = 20 μm, measured at temperatures T = 17.8 K, 25.9 K, 30.2 K, and 39.3 K, all above the critical temperature of the Nb film. An asymmetry with respect to V = 0 with a shift of the maximum about 10 mV can be seen, which can be explained by the influence of LMO ferromagnetism on the tunneling characteristics of MHS [17].

Although the resistivity of the single LMO film is significantly higher than that of the LCMO film at reduced temperatures, the resistance of the MHS with an LMO layer is significantly lower than the calculated R'_M contribution. With a further decrease in temperature to T = 6 K, which is already below the superconducting transition temperature of the Nb film the singularity feature of resistance with a minimum at V = 0 is manifested more clearly. However, the question whether it relates to the

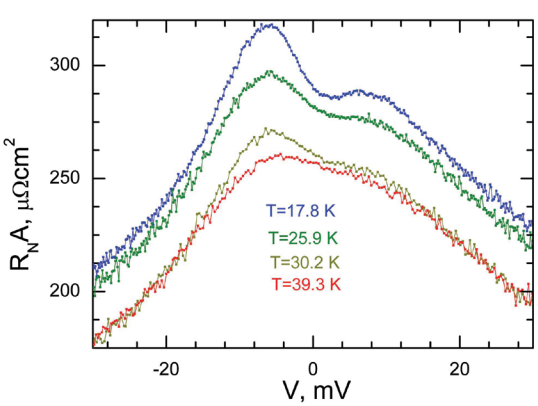

Fig. 1. *Family of characteristic resistivity dependences $R_N A(V)$ for MHS with LMO layer of thickness d_M = 6 nm and L = 20 μm, measured at temperatures T = 17.8 K, 25.9 K, 30.2 K and 39.3 K, which are higher than the critical temperature of the Nb film.*

appearance of superconducting current remained open.

Measurements at lower temperatures are shown in **Fig. 2**, which shows $R_N A(V)$ dependences for MHS, taken at $T < 4.2$ K. At low temperatures, the *M*-layer contribution from the LCMO to the MHS resistance is small due to the metal-insulator transition of the LCMO film. For the case of LMO film, on the contrary, as mentioned above, there is an increase in R'_M resistance with decreasing temperature, but the $R_{M/Y}$ contribution is more significant because the transparency *D* of the LCMO/YBCO and LMO/YBCO interface is smaller than for Au/LCMO or Au/LMO.

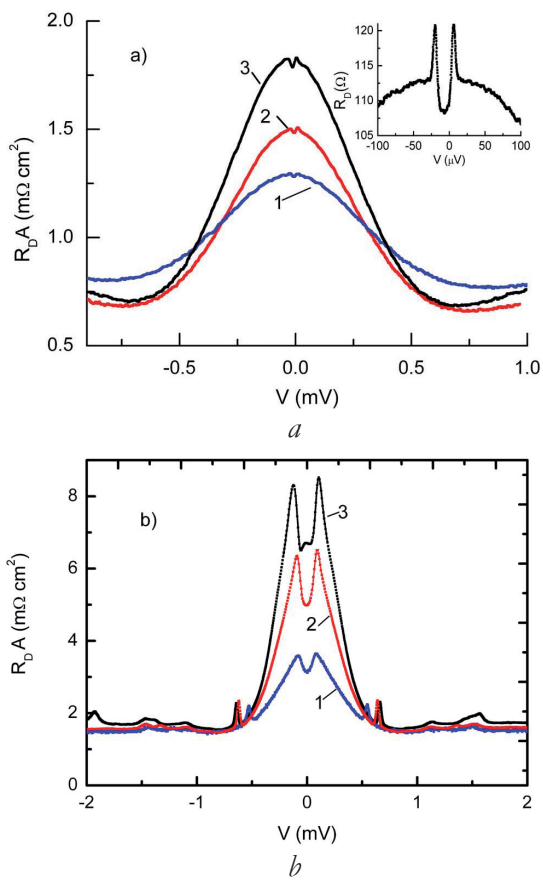

a

b

Fig. 2. *Family of dependences of RNA(V) at the temperatures T = 2 K, 1 K and 0.3 K for (a) MHS with LMO interlayer d_M = 6 nm, the inset shows a more detailed dependence at T = 0.3 K; (b) MHS with LCMO interlayer with thickness d_M = 20 nm.*

So, we are dealing with the structures with two low transparent barriers, which can strongly suppress the superconducting current (or critical I_C current) in proportion to the square of the D_2 transparency. The absence of superconducting current is indicated by the dependence $R_D(V)$ shown in the inset in Fig. 2*a*. It can be seen that even at $T = 0.3$ K there is an increase in resistance at $V = 0$, and low-energy sub-gap features on the dependence $R_D(V)$ distinctly registered.

It is possible to evaluate the influence of exchange interaction by values of the normalized conductivity ratio σ_0/σ_N, where σ_0 is taken at $V = 0$, and σ_N corresponds to conductivity of MHS in the normal conducting state. **Fig. 3** shows the temperature dependences of experimental values for σ_0/σ_N, taken from data on Fig. 2 and calculated using approach [14] taking values of exchange interaction $h = 0.1$ and $h = 1$ at fixed all other parameters of modeling. From Fig. 3 one may conclude that the

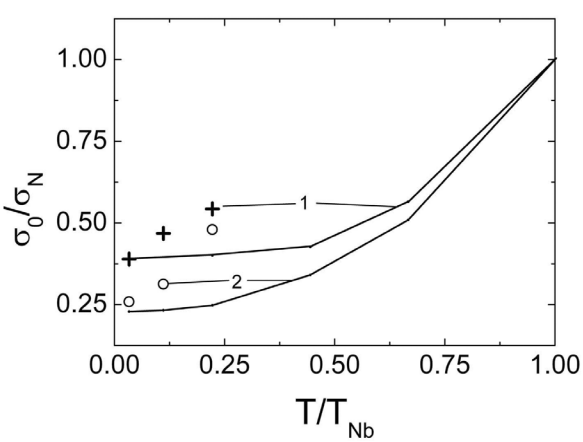

Fig. 3. *Temperature dependence of the normalized conductivity σ_0/σ_N at V = 0 for MHS with LMO (1) and LCMO (2) interlayers. Experiment: crosses (LMO), light circles (LCMO), theoretical curves correspond to exchange energy h = 0.1 (1) and h = 1 (2).*

ferromagnetism in the LMO layer is much weaker than in the LCMO.

3.2. Characteristics of MHS with $Ca_xSr_{1-x}CuO_2$ antiferromagnetic layer

Replacement of the ferromagnetic interlayer with an antiferromagnetic one is manifested in appearance of a superconducting current. **Fig. 4** shows the temperature dependence of the resistance of three MHS with *M* layer made of $Ca_{0.5}Sr_{0.5}CuO_2$ (CSCO) for different interlayer thicknesses d_M = 80, 50, and 20 nm. The inset on the same figure shows the superconducting transition for the MHS with d_M = 20 nm.

The superconducting current I_C was observed at T = 4.2 K for MHS with interlayer thickness up to d_M = 50 nm, detectable by the differential conductivity peak on the dependence of $R_D(V)$ at $V = 0$. In contrast to the manganite interlayers characterized by the nonzero energy of exchange interaction $h > 0$, in the case of the antiferromagnetic (AF) interlayer, the main contribution to the reduction of the superconducting current comes from the transparency of the Au/CSCO and YBCO/CSCO barriers. We consider that the barrier thickness condition for existence of superconducting current is satisfied as for the case of *S/N/S* junctions, when I_C exponentially decreases with the ratio d_N/ξ_N (ξ_N is the coherence length in the normal metal interlayer).

Thus, MHS can be considered as $S_d/M/S$ structures, where S_d is a YBCO electrode with a dominant *d*-wave order parameter, *S* is a superconducting Nb/Au bilayer (due to the strong proximity effect in thin Au film of thickness $d_{Au} < l$, smaller than the free path length l).

Fig. 5 shows a simplified model for YBCO/CSCO/Au/Nb MHS in which the antiferromagnetic interlayer is represented as a normal metal with an antiferromagnetic ordering N(AF) and the CSCO/Au barrier with transparency $D < 1$ is an insulator with thickness d_0 and dielectric permittivity ε. The barrier layer in the inset is given as white gap between the CSCO and Au films, in which there is

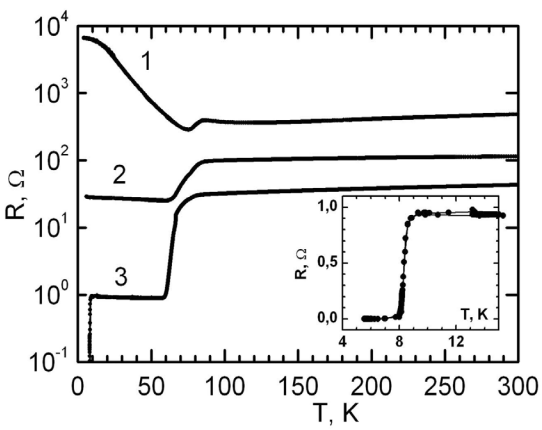

Fig. 4. *Temperature dependence of the resistance of three MHS with CSCO. The curve (1) corresponds to d_M = 80 nm, (2) d_M = 50 nm, (3) d_M = 20 nm. The inset shows the transition to the superconducting state of MHS (3).*

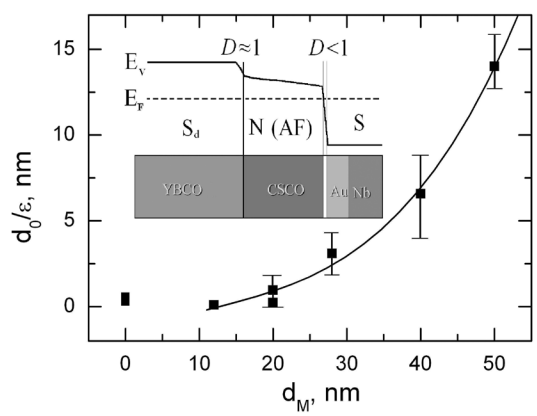

Fig. 5. *Dependence of the barrier parameter d_0/ε vs. the CSCO layer thickness d_M. The inset shows the band diagram for the YBCO/CSCO/Au/Nb hybrid mesa-heterostructure with different values of interface transparency D. The E_V energy denotes the valence zone, and the E_F is the Fermi energy shown as a dashed line.*

drown an abrupt change in the energy level E_V characterizing the valence zone. As can be seen from Fig. 5, the parameter d_0/ε grows exponentially with thickness d_M, calculated from the capacity $C = A\varepsilon/4\pi d_0$ of the MHS, which was estimated from the hysteresis of I-V characteristics which were observed in experiment.

4. CONCLUSION

Hybrid planar mesa-heterostructures with three types of the oxide barrier layer epitaxially grown on top of the $YBa_2Cu_3O_x$ cuprate superconductor were experimentally studied, and the Au/Nb bilayer was used as the upper superconducting electrode. In the case of a barrier layer of ferromagnetic manganite $La_{0.7}Ca_{0.3}MnO_3$ or $LaMnO_3$ the exchange interaction prevented flow of superconducting current even when the mesa-heterostructures were cooled to temperature $T = 0.3$ K and the layer thickness was reduced to $d_M = 6$ nm - a value which guarantees the absence of pinholes. In the case of the $Ca_{0.5}Sr_{0.5}CuO_2$ antiferromagnetic cuprate interlayer, superconducting current was detected at $T = 4.2$ K increasing the interlayer thickness up to $d_M = 50$ nm. At low temperatures $T < 4.2$ K, the dependences of differential resistance vs. voltage for mesa-heterostructures with manganite interlayers exhibited features which could be attributed to the appearance of low-energy sub-gap states.

REFERENCES

1. Fulde P and Ferrell RA. Superconductivity in a strong spin-exchange field. *Phys.Rev.*, 1964, 135:A550-A563.
2. Larkin AI and Ovchinnikov YN. Inhomogeneous state of superconductors. *Sov.Phys.JETP*, 1965, 20:762-769.
3. Bulaevskii LN, Kuzii VV, and Sobyanin AA. Superconducting system with weak coupling with a current in the ground state. *JETP Lett.*, 1977, 25:290-294.
4. Ryazanov VV, Oboznov VA, Rusanov AYu, Veretennikov AV, Golubov AA, and Aarts J. Coupling of two superconductors through a ferromagnet: Evidence for a π-junction. *Phys.Rev.Lett.*, 2001, 86:2427-2430.
5. Buzdin AI. Proximity effects in superconductor-ferromagnet heterostructures. *Rev.Mod.Phys.*, 2005, 77(3):935-976.
6. Bergeret FS, Volkov AF, Efetov KB. Odd triplet superconductivity and related phenomena in superconductor-ferromagnet structures. *Rev.Mod.Phys.*, 2005, 77(4):1321-1373.
7. Gor'kov L, Kresin V. Giant magnetic effects and oscillations in antiferromagnetic Josephson weak links. *Appl.Phys.Lett.*, 2001, 78(23):3657-3659.
8. Zaitsev AV. Peculiarities of the proximity effect in superconductor-multilayered ferromagnet structures with collinear magnetizations in ferromagnetic layers. *JETP Lett.*, 2009, 90(6):475-479.
9. Zaitsev AV, Ovsyannikov GA, Constantinian KY, Kislinskii YV, Shadrin AV, Borisenko IV and Komissinskiy PV. Superconducting current in hybrid structures with an antiferromagnetic interlayer. *JETP*, 2010, 110(2):336-344.
10. Dorr K. Ferromagnetic manganites: spin-polarized conduction versus competing interactions. *J.Phys.D: Appl. Phys.*, 2006, 39:R125-R150.
11. Pena V, Sefrioui Z, Arias D, Leon C, Santamaria J, Varela M, Pennycook SJ and

Martinez JL. Coupling of superconductors through a half-metallic ferromagnet: Evidence for a long-range proximity effect. *Phys.Rev.B*, 2004, 69(22):224502.

12. Moran O, Bacab E, Perez FA. Depression of the superconducting critical temperature and finite-size scaling relation in $YBa_2Cu_3O_{7-\delta}/La_{2/3}Ca_{1/3}MnO_3$ bilayers. *Microelectronics Journal,* 2008, 39(3-4):556-559.
13. Salamon MB, Jaime M. The physics of manganites: Structure and transport. *Rev. Mod.Phys.*, 2001, 73(3):583-628.
14. Petrzhik AM, Ovsyannikov GA, Shadrin AV, Konstantinyan KI, Zaitsev AV, Demidov VV, and Kislinskii YuV. Electron Transport in Hybrid Superconductor Heterostructures with Manganite Interlayers. *JETP*, 2011, 12 (6):1042-1050.
15. Ovsyannikov GA, Constantinian KY, Kislinskii YuV, Shadrin AV, Zaitsev AV, Petrzhik AM, Demidov VV, Borisenko IV, Kalaboukhov AV, and Winkler D. Proximity effect and electron transport in oxide hybrid heterostructures with superconducting/magnetic interfaces. *Supercond. Sci. Technol.*, 2011, 24(5): 055012.
16. Komissinskiy PV, Ovsyannikov GA, Constantinian KY, Kislinskii YuV, Borisenko IV, Soloviev II, Kornev VK, Goldobin E and Winkler D. High-frequency dynamics of hybrid oxide Josephson heterostructures. *Phys.Rev.B*, 2008, 78(2):024501.
17. Ovsyannikov GA, Kislinskii YuV, Constantinian KY, Shadrin AV, Demidov VV, and. Petrzhik AM. Spin-Filter Tunneling in Superconducting Mesa Structures with a Ferromagnetic Manganite Interlayer. *JETP*, 2017, 124(4):628-634.